CNRS
Centre National de la Recherche Scientifique

INFN
Istituto Nazionale di Fisica Nucleare

Advanced Virgo Length Sensing and control: Double demodulation vs Single demodulation

VIR-069B-08

Gabriele Vajente
INFN sezione di Pisa and Pisa University

Issue: 1

Date: October 14, 2008

VIRGO * A joint CNRS-INFN Project
Via E. Amaldi, I-56021 S. Stefano a Macerata - Cascina (Pisa)
Secretariat: Telephone (39) 050 752 521 * FAX (39) 050 752 550 * Email W3@virgo.infn.it

Contents

1 Introduction **1**

2 Advantages and Dis-advantages **1**

3 Noise performances **2**

4 Radiation pressure effects **4**

5 Conclusions **6**

A Radiation pressure effects in the single demodulation scheme **7**

B Radiation pressure effects in the double demodulation scheme **12**

1 Introduction

The goal of this note is to compare the implementation and noise performances of the Advanced Virgo length sensing and control system in the single and double demodulation schemes:

- the *single demodulation* scheme is the straightforward extension of the Virgo signal extraction scheme: all demodulation happens at single modulation frequencies, thus extracting the beating between the carrier and a pair of RF sidebands. All sidebands must be generated with phase-modulation.
- in the *double demodulation* scheme instead the error signals for the short degrees of freedom are extracted by demodulating at the sum or difference of two modulation frequencies, thus extracting the beating between two pairs of sidebands.

The following results have been obtained using the Optickle simulations already explained in [3].

2 Advantages and Dis-advantages

The main advantage of the double demodulation scheme is the intrinsic decoupling of short degrees of freedom from the carrier field. This means that the coupling of DARM and CARM motion to MICH / PRCL / SREC is largely reduced. Indeed in the single demodulation scheme, almost all error signals are dominated by large factors by DARM and CARM contributions. In Virgo this problem has been tackled by ensuring a gain hierarchy. The SSFS had very high gain inside all other loop active bands, thus reducing the amount of CARM signal present in the other error signals. This ensured a closed-loop decoupling of frequency noise from the other d.o.f.s. In a similar way DARM had a large gain inside the MICH band-width, ensuring again a closed-loop decoupling.

Moreover, radiation pressure effects induce complex frequency dependences of the optical matrix, which change accordingly to the laser input power. As explained in the previous note [3], these effects affect mainly the carrier field, and therefore double demodulated signals are almost immune to it, while all single demodulated signals are strongly affected. More details are given in sec. 4.

The main dis-advantage of the double demodulation technique is the reduced signal to noise ratio due to the smaller amplitude of RF fields. Indeed single demodulated signals are proportional to $J_0(m)J_1(m) \sim \frac{m}{2}$ instead of $J_1(m)J_1(m) \sim \frac{m^2}{4}$. Moreover double demodulation needs amplitude modulation and it is not yet clear if this is compatible with the angular sensing and control system.

In general the use of a single demodulation scheme seems the simplest extension of the present Virgo scheme, even if its implementation in high-power Advanced Virgo might turn out to be difficult because of radiation-

D.O.F.	Signals	Compensation		Control		UGF
		Zeros	Poles	Zeros	Poles	
DARM	ASY_DC	(-39,10)	(0.6,5)	(1,0) (10,1) (30,1) (315,0) (600,0)	(0,0.7) (0.5,1) (300,1), (874,0.7)	60
CARM	SYM_SB1_P	(4.33,6) (25500,7) (50000,750)	(0.55,10) (25500,10) (50000,1)		(0,0)	23000
PRCL	SYM_SB3_P	(0.61,72) (-3.36,0) (3.98,0) (4.35,5.4)	(0.587,0) (0.625,9.1) (1.82,23.1) (26.44,0)	(3,0) (10,1)	(0,0.7) (300,1) (500,1)	40
MICH	SYM_SB2_Q			(3,0) (7,1)	(0,0.7) (100,1) (200,1)	20
SREC	SYM_SB1_P	(0.615,318) (3.28,0) (4.31,6.1) (10.18,0)	(0.622,478) (7.27,0) (7.45,10.8) (7.59,0)	(3,0) (7,1)	(0,0.7) (100,1) (200,1)	20

Table 1: Control loops parameters. Poles and zeros are written in the (f,Q) form.

pressure driven effects. However, the foreseen extension of the Virgo locking scheme, briefly explained in [1, 2], does not need double demodulation to be implemented, unlike Advanced LIGO locking scheme.

3 Noise performances

The longitudinal control performances in terms of noise re-injected in the gravitational channel have already been studied for the double demodulation scheme. The result, taken from [3], is reported for reference in the top panel of fig. 1. As stated in [3], the auxiliary loop noises can be brought below the design sensitivity with the implementation of noise subtraction techniques capable of a cancellation factor of about 100. Since in Virgo a factor of about 1000 has been stably reached for the dominant noise source, this seems not a difficult task

A similar simulation can be carried out in the single demodulation scheme. DARM and CARM controls are unchanged with respect to the other situation, being locked respectively on ASY_DC and SYM_SB1_P. The best error signals for MICH, PRCL and SREC turned out to be respectively: SYM_SB2_Q, SYM_SB3_P and SYM_SB2_P. The optical transfer functions for these signals are shown in fig. 2.

For PRCL and SREC the control filters consist in two parts: a first compensation filter to remove most of the radiation-pressure-induced frequency dependence, and the main control filter. The parameters for the filters are listed in tab. 1.

The resulting noise re-introduced in the gravitation channel is shown in the bottom panel of fig. 1. The results are very interesting, since it turns out that the auxiliary loop quantum noise is re-introduced at a level which is quite close to the design sensitivity. Therefore the requirements for noise subtractions are less stringent in this configuration than in the double demodulation one.

However, the contribution of CARM noise is much larger in the single demodulation scheme. It is easy to prove that the coupling path passes through PRCL and SREC loops. Indeed, if the PRCL locking loop is switched off, the CARM contribution changes around 100-200 Hz, and switching off the SREC loop it significantly reduces below 200 Hz. Even if the direct coupling of CARM noise to the gravitational channel is the same in both single and double demodulation schemes, the use of single demodulation increases the coupling to the auxiliary

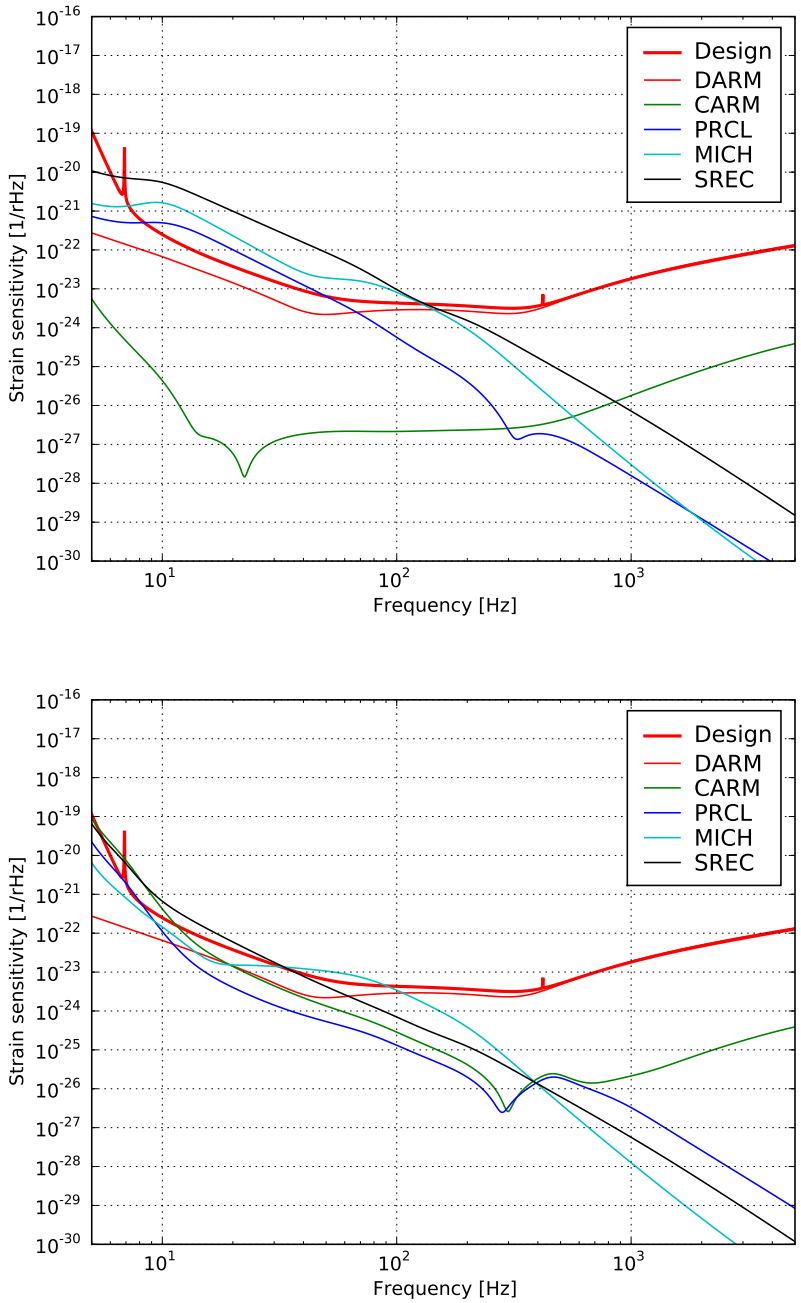

Figure 1: Noise re-introduced in the gravitational channel by the length sensing and control system, in the double (top) and single (bottom) demodulation schemes.

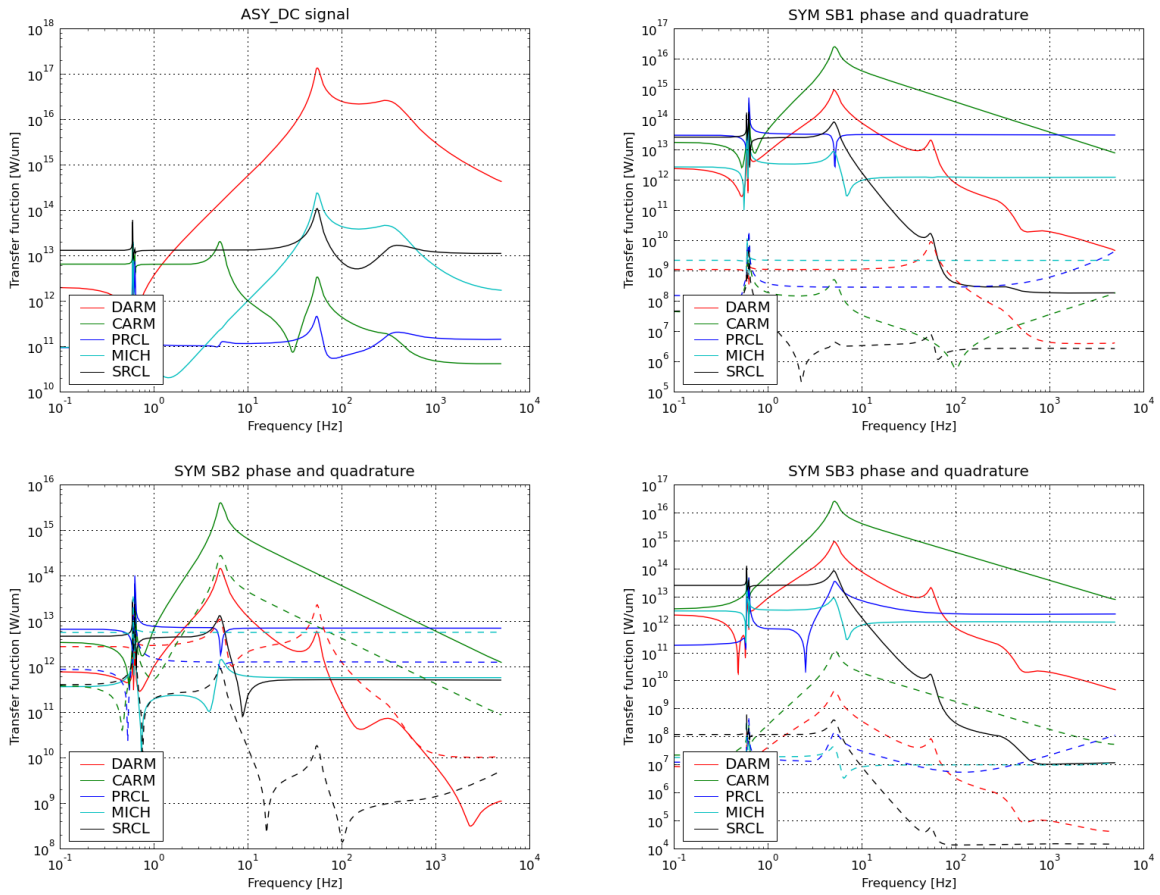

Figure 2: Optical transfer functions, in the single demodulation scheme, for the signals used in the longitudinal control system.

channels and therefore the indirect coupling to the output channel. This situation will benefits from the noise subtraction of PRCL and SREC, but it can also be improved using other subtraction paths: CARM signal can be subtracted from PRCL and SREC one to reduce the noise.

However, the reduction of noise re-introduction using the single demdolation scheme is not very large and less than a factor 10 at almost all frequencies. An improvement in the signal to noise ratio in the double demodulation scheme can be obtained increasing the modulation index. Indeed in the simulations described so far, all modulation indices was set to 0.1. If every modulation is doubled in amplitude, the signal will be 4 times larger. Since the SYM noise is mainly dominatd by the carrier reflected power, the quantum noise will remain more or less the same. Therefore there will be a neat gain of a factor 4 in noise reduction. A example of the resulting performances with doubled modulation index is shown in fig. 3.

4 Radiation pressure effects

To have a more extensive characterization of radiation pressure effects in the optical matrix, full simulations have been carried out both in the single and double demodulation scheme, varying the input power: almost 0 W, 3 W, 8 W, 25 W, 50 W and 125 W. All transfer functions have been rescaled to full power to make the comparison simpler.

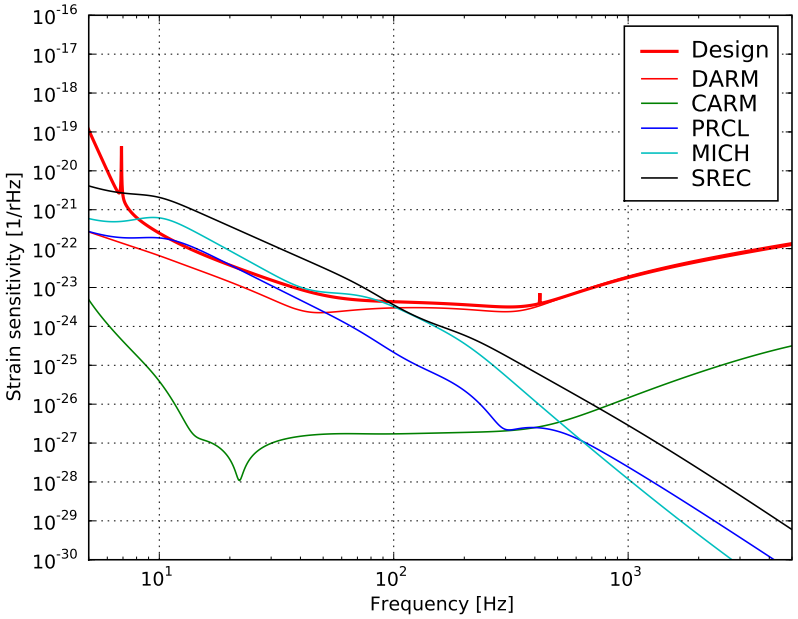

Figure 3: Noise re-introduced in the gravitational channel by the length sensing and control system, in the double demodulation scheme with modulation index set to 0.2 instead of 0.1.

D.O.F.	Single demodulation	Double demodulation
DARM	ASY_DC	ASY_DC
CARM	SYM_SB1_P	SYM_SB1_P
PRCL	SYM_SB3_P	SYM_3P1_P
MICH	SYM_SB2_Q	SYM_2M1_Q
SREC	SYM_SB1_P	SYM_2M1_P

Table 2: Error signals used in the single and double demodulation scheme.

The effect on all error signal are shown in appendix A for the single demodulation scheme and in appendix B for the double demodulation one. Table 2 just recall the error signal used in both schemes.

As already pointed out, in the double demodulation scheme the error signals used for the central interferometer are almost not affected by radiation pressure. The transfer function from each short d.o.f. to the corresponding error signal is flat at any input power, showing only negligible changes. What changes mostly is the coupling of CARM and DARM motion to the central interferometer error signals and the out of diagonal terms in the optical matrix. These effects are not very important from the controllability point of view, but they can increase the amount of noise re-introduced by the controls. This can be solved implementing suitable off-diagonal sensing terms, which should be frequency dependent. Even if the implementation of these terms closely resembles the compensation filters needed in the single demodulation scheme, they will be of a much simpler implementation, since they are not critical for maintaining the lock.

In the single demodulation scheme radiation pressure effects are indeed very large and they change completely the shape of all transfer function at low frequency. The implementation of an input power dependent compensation seems difficult, taking also into account that these compensations are critical for maintaining the stability of the lock.

5 Conclusions

From the above analysis, it seems clear that:

- the double demodulation scheme allows to reach quite good performances in terms of noise re-introduction. Noise subtraction techniques must be implemented and need cancellation factors of at most 100. Only CARM and DARM loops need a power-dependent compensation filter, since the short degrees of freedom are almost radiation pressure free.
- the single demodulation scheme gives better performances in terms of noise re-introduction, since control noise is at most a factor 10 above the design sensitivity. However all loops except MICH must include power-dependent compensations for radiation pressure effects.

A final remark is needed. All the above simulations assumed the error signals to be limited by quantum noise, and not by other sources of control or environmental noises. Such noises will couple in the same way in both configurations. One should consider carefully if environmental noise is expected to be lower in one of the two configurations: for example if the largest light scattering affects mainly the carrier field, the use of double demodulation might help in reducing the amount of extra noise in the auxiliary error signals.

In conclusion, it is not yet clear which of the two configuration is the best one. The single demodulation scheme seems much more promising in terms of noise performances, but the implementation of the needed compensations seems not a simple task. It might pay to adopt the double demodulation scheme, at the price of a bit more of noise, since the implementation is simpler.

A Radiation pressure effects in the single demodulation scheme

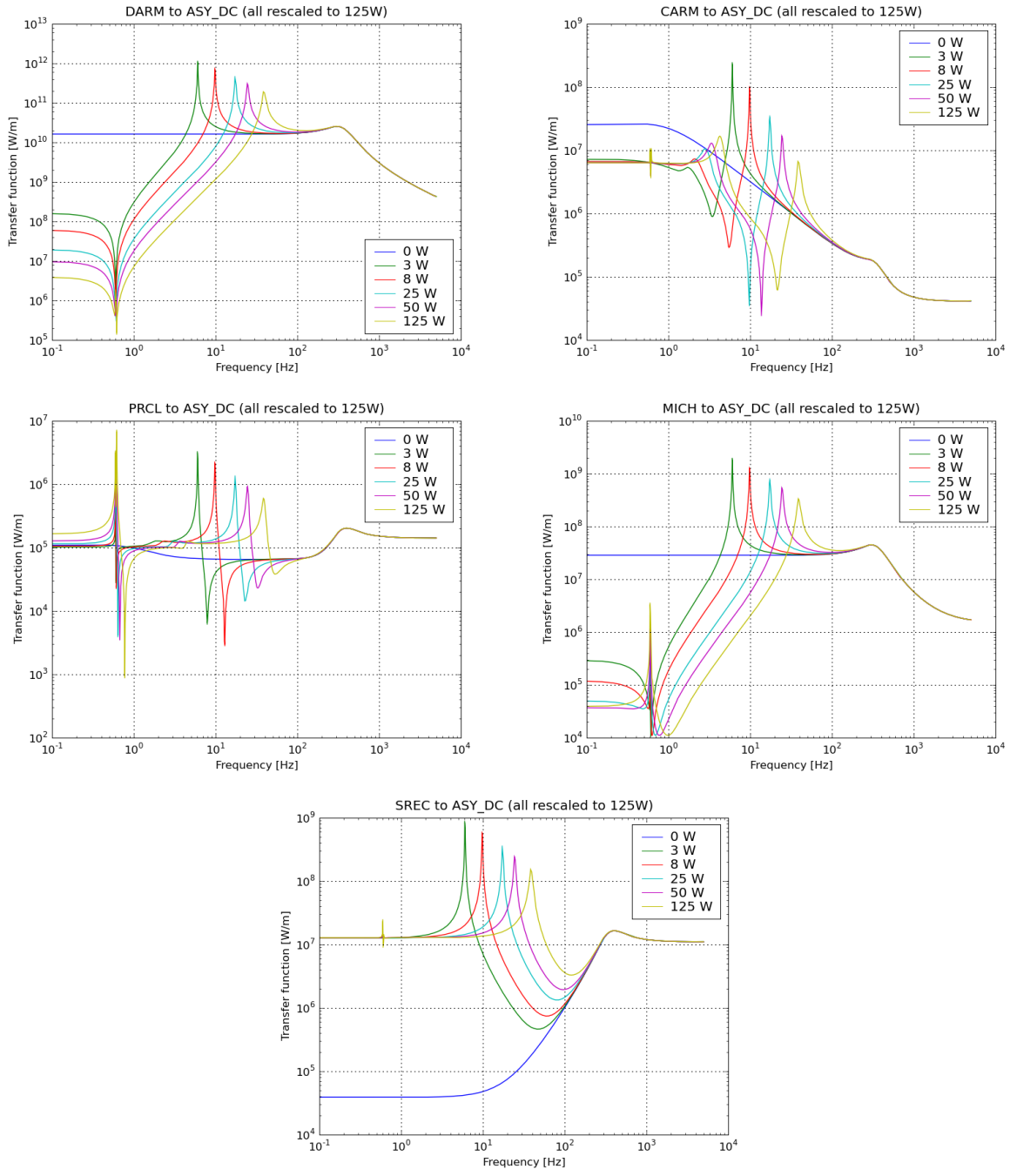

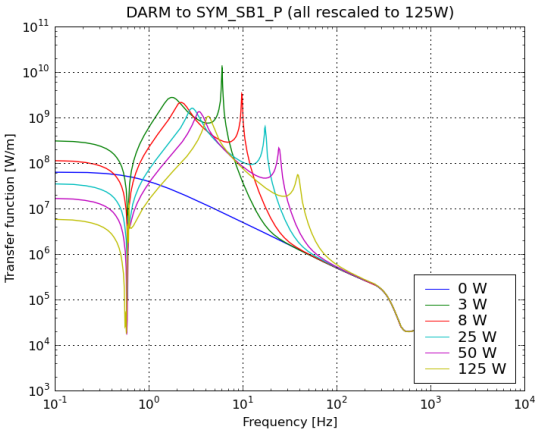
DARM to SYM_SB1_P (all rescaled to 125W)
Transfer function [W/m]
Frequency [Hz]
0 W
3 W
8 W
25 W
50 W
125 W

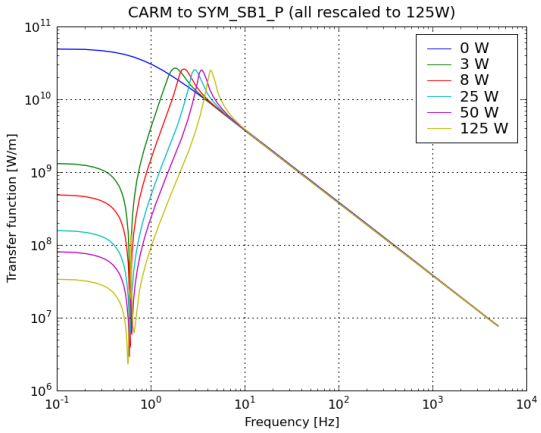
CARM to SYM_SB1_P (all rescaled to 125W)
Transfer function [W/m]
Frequency [Hz]
0 W
3 W
8 W
25 W
50 W
125 W

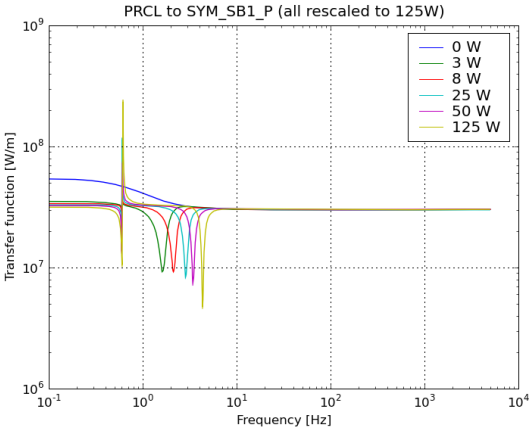
PRCL to SYM_SB1_P (all rescaled to 125W)
Transfer function [W/m]
Frequency [Hz]
0 W
3 W
8 W
25 W
50 W
125 W

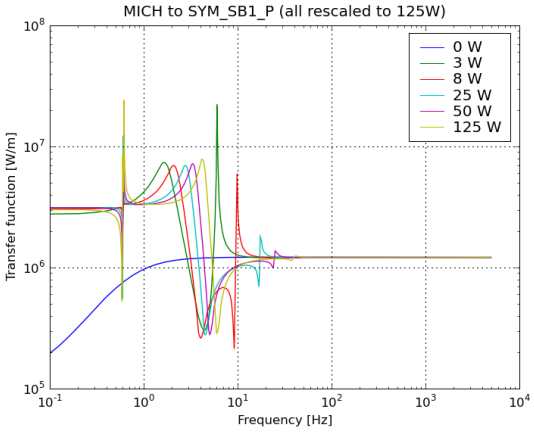
MICH to SYM_SB1_P (all rescaled to 125W)
Transfer function [W/m]
Frequency [Hz]
0 W
3 W
8 W
25 W
50 W
125 W

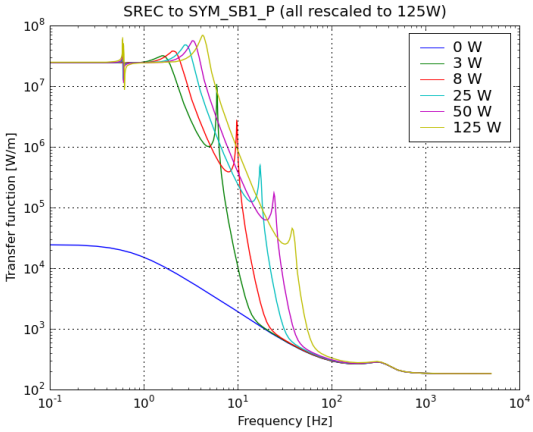
SREC to SYM_SB1_P (all rescaled to 125W)
Transfer function [W/m]
Frequency [Hz]
0 W
3 W
8 W
25 W
50 W
125 W

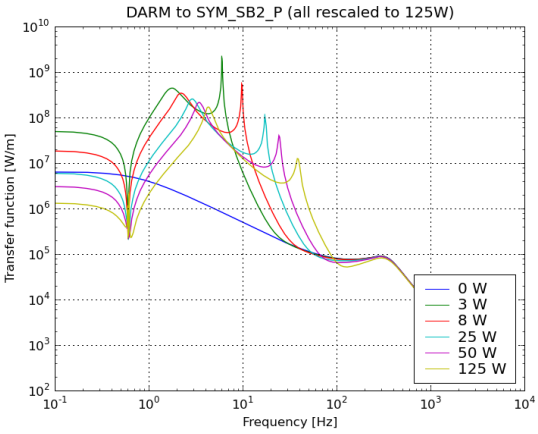
DARM to SYM_SB2_P (all rescaled to 125W)
Transfer function [W/m]
Frequency [Hz]
0 W
3 W
8 W
25 W
50 W
125 W

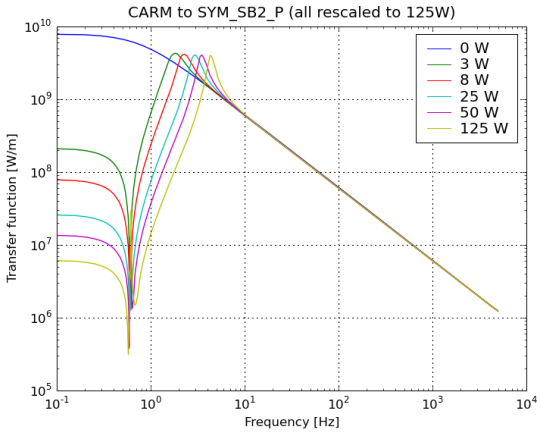
CARM to SYM_SB2_P (all rescaled to 125W)
Transfer function [W/m]
Frequency [Hz]
0 W
3 W
8 W
25 W
50 W
125 W

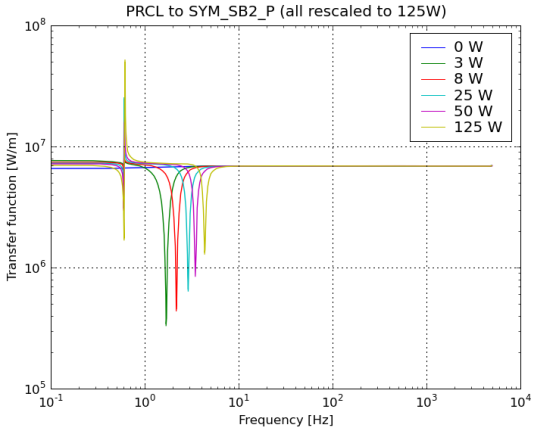
PRCL to SYM_SB2_P (all rescaled to 125W)
Transfer function [W/m]
Frequency [Hz]
0 W
3 W
8 W
25 W
50 W
125 W

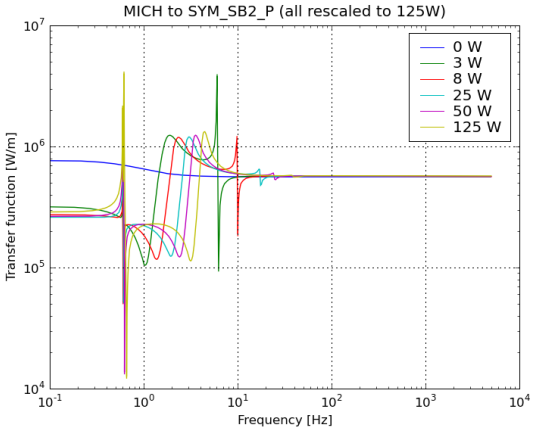
MICH to SYM_SB2_P (all rescaled to 125W)
Transfer function [W/m]
Frequency [Hz]
0 W
3 W
8 W
25 W
50 W
125 W

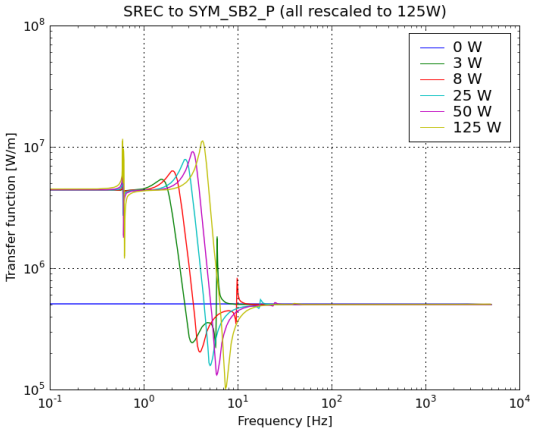
SREC to SYM_SB2_P (all rescaled to 125W)
Transfer function [W/m]
Frequency [Hz]
0 W
3 W
8 W
25 W
50 W
125 W

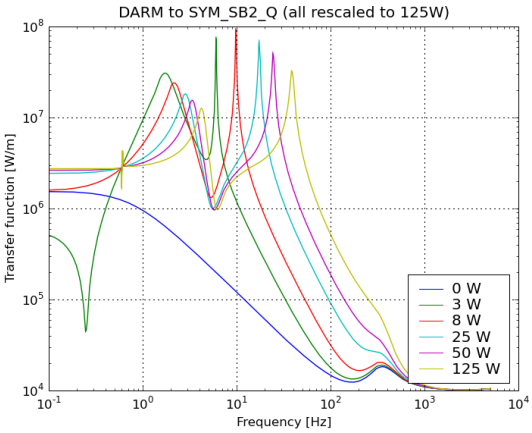
DARM to SYM_SB2_Q (all rescaled to 125W)
Transfer function [W/m]
Frequency [Hz]
0 W
3 W
8 W
25 W
50 W
125 W

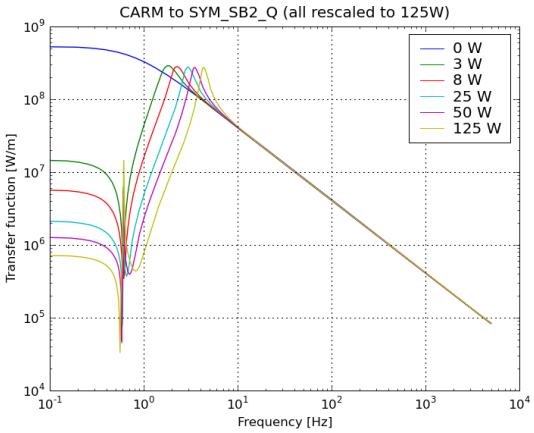
CARM to SYM_SB2_Q (all rescaled to 125W)
Transfer function [W/m]
Frequency [Hz]
0 W
3 W
8 W
25 W
50 W
125 W

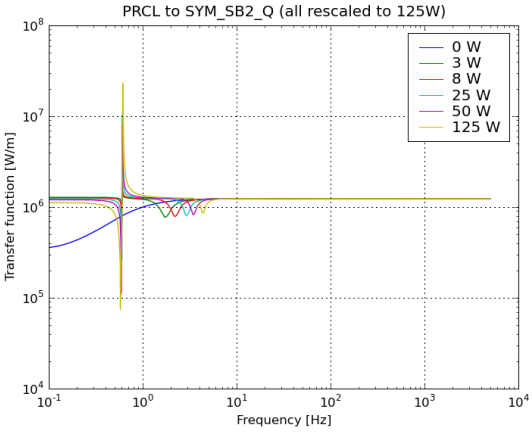
PRCL to SYM_SB2_Q (all rescaled to 125W)
Transfer function [W/m]
Frequency [Hz]
0 W
3 W
8 W
25 W
50 W
125 W

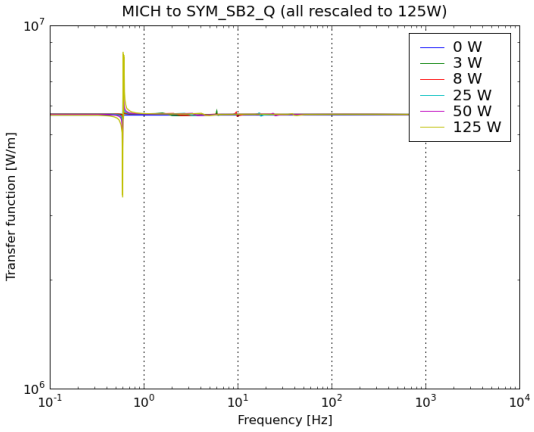
MICH to SYM_SB2_Q (all rescaled to 125W)
Transfer function [W/m]
Frequency [Hz]
0 W
3 W
8 W
25 W
50 W
125 W

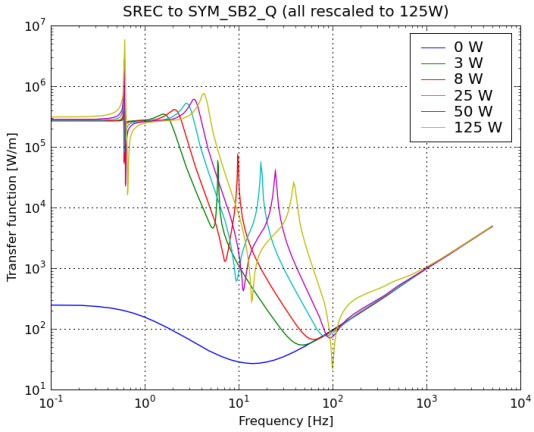
SREC to SYM_SB2_Q (all rescaled to 125W)
Transfer function [W/m]
Frequency [Hz]
0 W
3 W
8 W
25 W
50 W
125 W

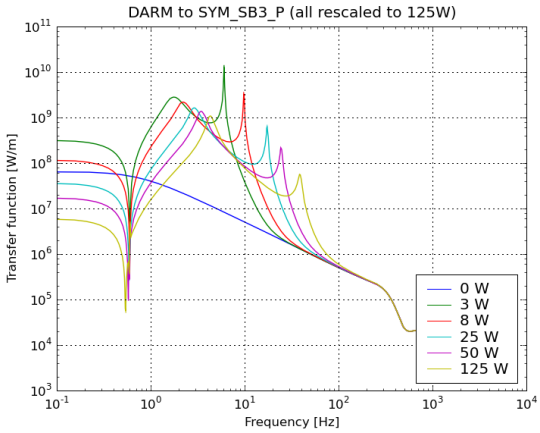
DARM to SYM_SB3_P (all rescaled to 125W)
Transfer function [W/m]
Frequency [Hz]
0 W
3 W
8 W
25 W
50 W
125 W

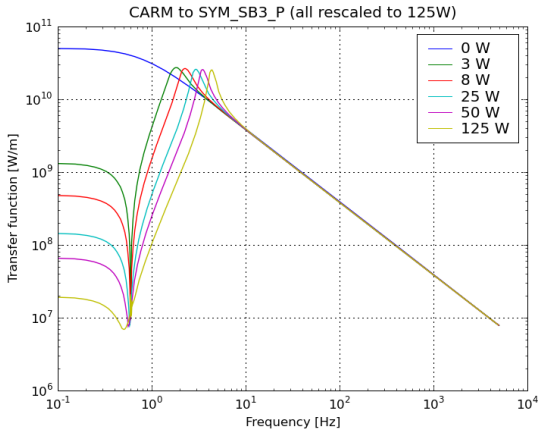
CARM to SYM_SB3_P (all rescaled to 125W)
Transfer function [W/m]
Frequency [Hz]
0 W
3 W
8 W
25 W
50 W
125 W

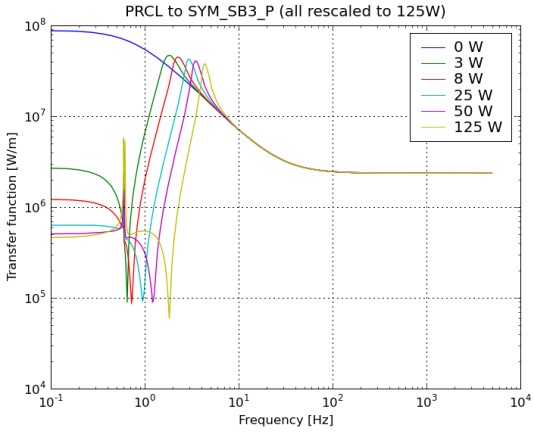
PRCL to SYM_SB3_P (all rescaled to 125W)
Transfer function [W/m]
Frequency [Hz]
0 W
3 W
8 W
25 W
50 W
125 W

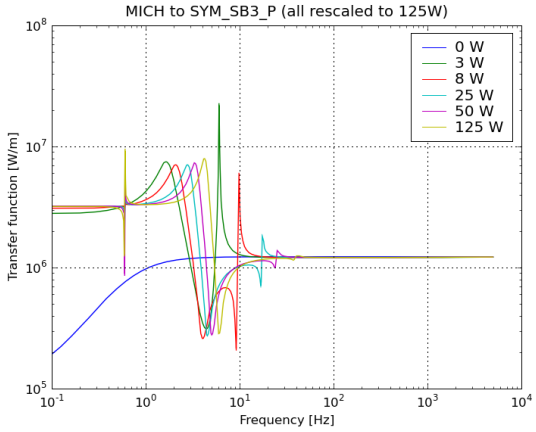
MICH to SYM_SB3_P (all rescaled to 125W)
Transfer function [W/m]
Frequency [Hz]
0 W
3 W
8 W
25 W
50 W
125 W

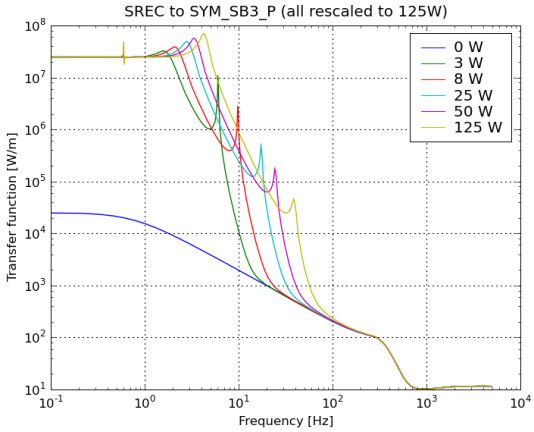
SREC to SYM_SB3_P (all rescaled to 125W)
Transfer function [W/m]
Frequency [Hz]
0 W
3 W
8 W
25 W
50 W
125 W

B Radiation pressure effects in the double demodulation scheme

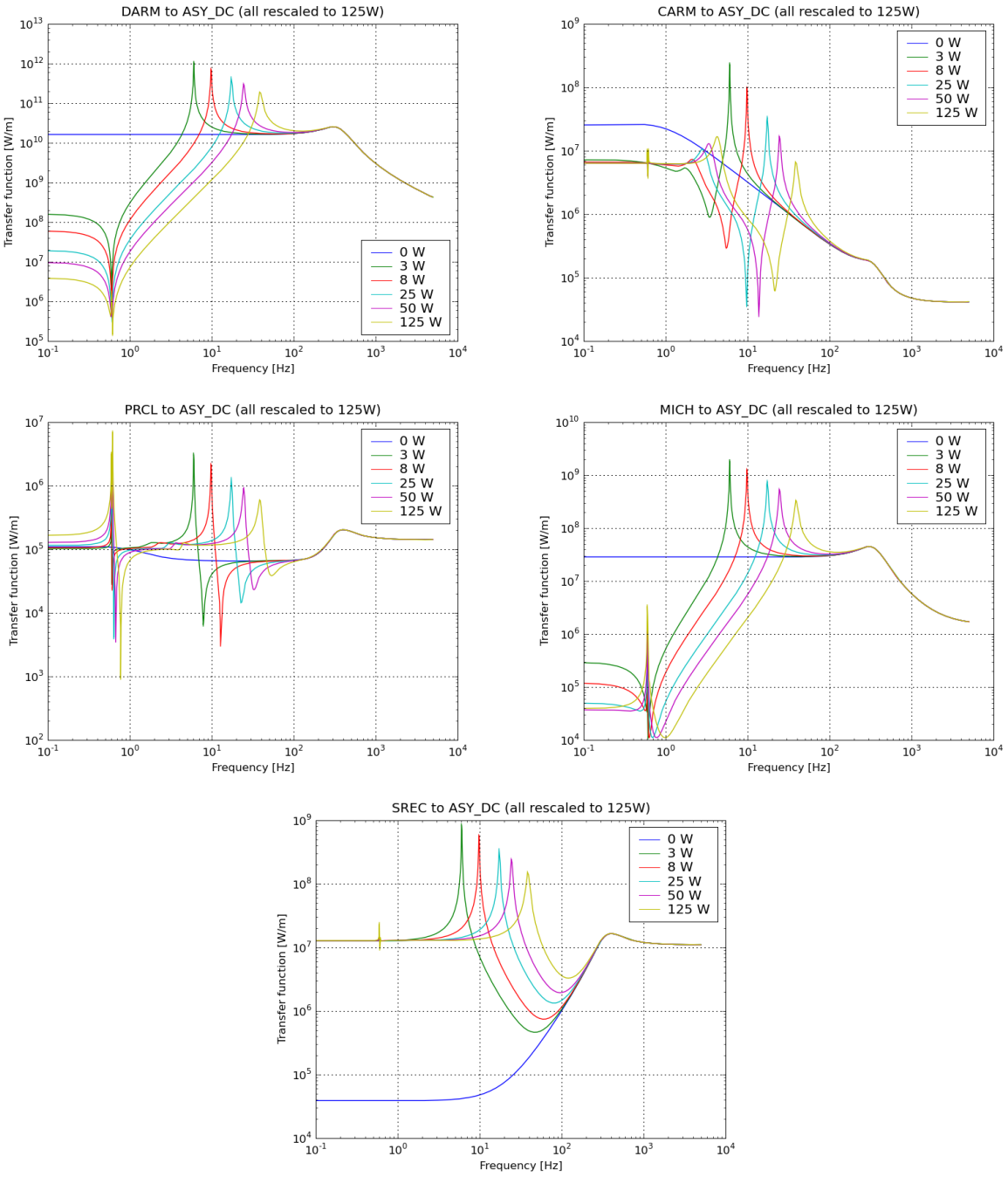

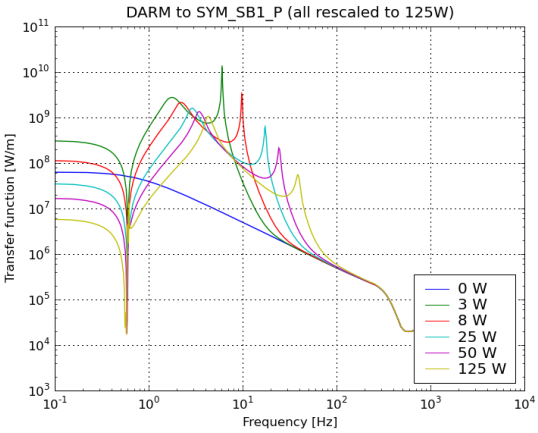
DARM to SYM_SB1_P (all rescaled to 125W)
Transfer function [W/m]
Frequency [Hz]
0 W
3 W
8 W
25 W
50 W
125 W

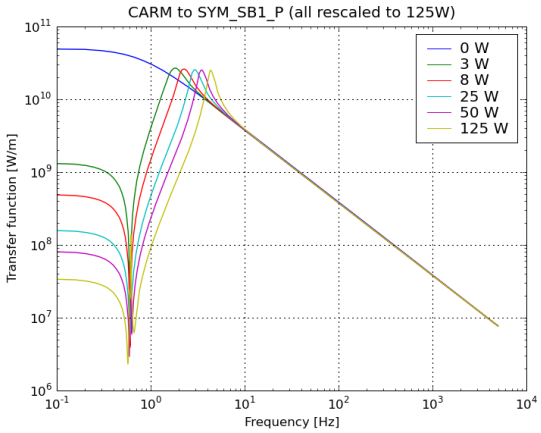
CARM to SYM_SB1_P (all rescaled to 125W)
Transfer function [W/m]
Frequency [Hz]
0 W
3 W
8 W
25 W
50 W
125 W

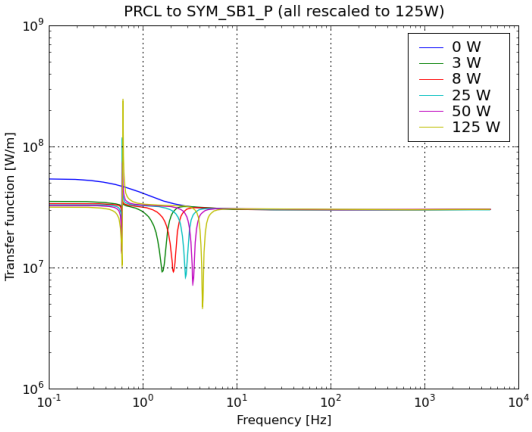
PRCL to SYM_SB1_P (all rescaled to 125W)
Transfer function [W/m]
Frequency [Hz]
0 W
3 W
8 W
25 W
50 W
125 W

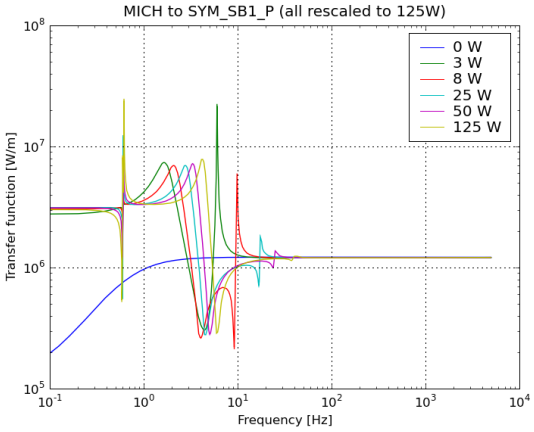
MICH to SYM_SB1_P (all rescaled to 125W)
Transfer function [W/m]
Frequency [Hz]
0 W
3 W
8 W
25 W
50 W
125 W

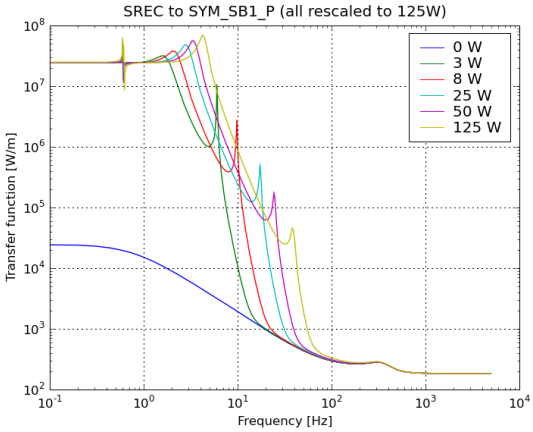
SREC to SYM_SB1_P (all rescaled to 125W)
Transfer function [W/m]
Frequency [Hz]
0 W
3 W
8 W
25 W
50 W
125 W

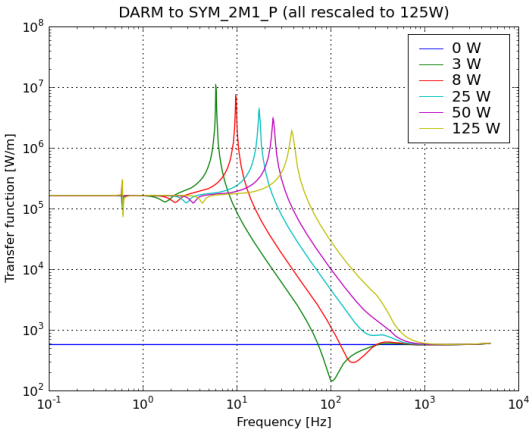
DARM to SYM_2M1_P (all rescaled to 125W)
Transfer function [W/m]
Frequency [Hz]
0 W
3 W
8 W
25 W
50 W
125 W

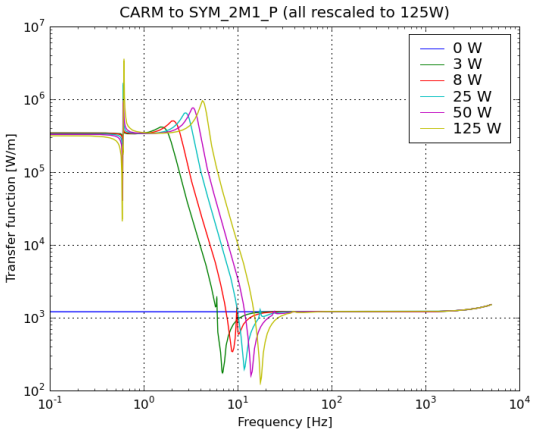
CARM to SYM_2M1_P (all rescaled to 125W)
Transfer function [W/m]
Frequency [Hz]
0 W
3 W
8 W
25 W
50 W
125 W

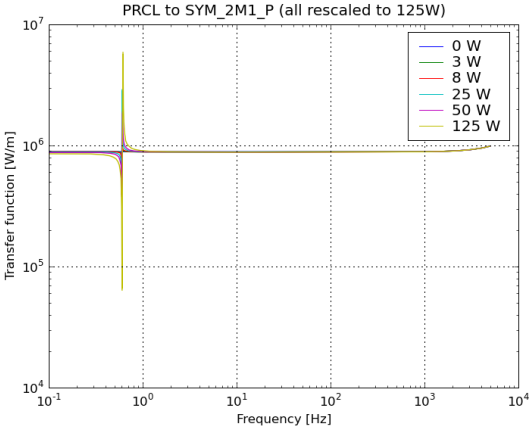
PRCL to SYM_2M1_P (all rescaled to 125W)
Transfer function [W/m]
Frequency [Hz]
0 W
3 W
8 W
25 W
50 W
125 W

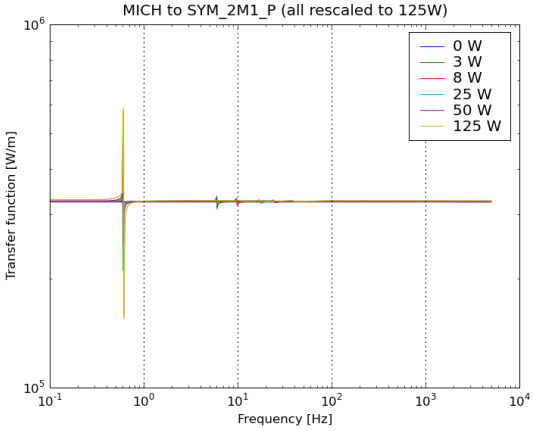
MICH to SYM_2M1_P (all rescaled to 125W)
Transfer function [W/m]
Frequency [Hz]
0 W
3 W
8 W
25 W
50 W
125 W

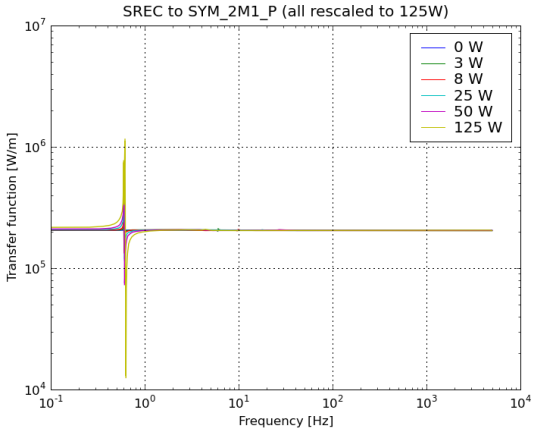
SREC to SYM_2M1_P (all rescaled to 125W)
Transfer function [W/m]
Frequency [Hz]
0 W
3 W
8 W
25 W
50 W
125 W

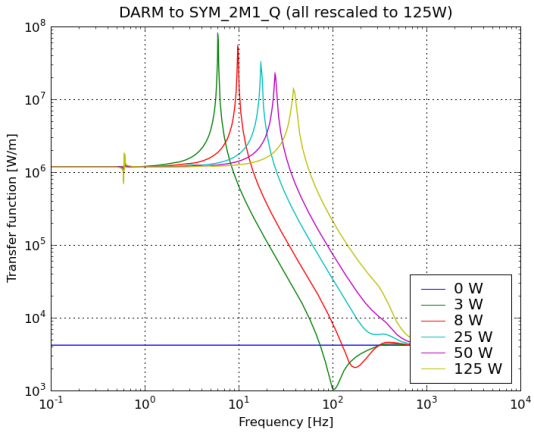
DARM to SYM_2M1_Q (all rescaled to 125W)
Transfer function [W/m]
Frequency [Hz]
0 W
3 W
8 W
25 W
50 W
125 W

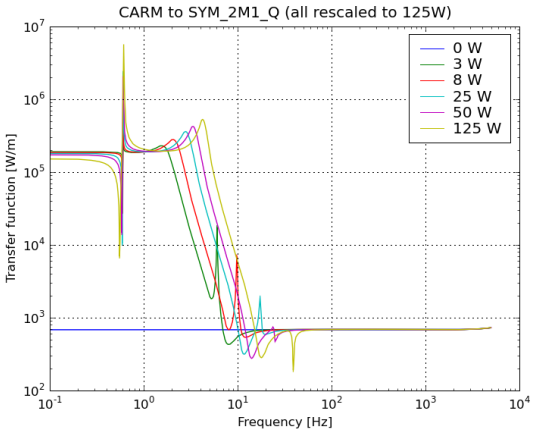
CARM to SYM_2M1_Q (all rescaled to 125W)
Transfer function [W/m]
Frequency [Hz]
0 W
3 W
8 W
25 W
50 W
125 W

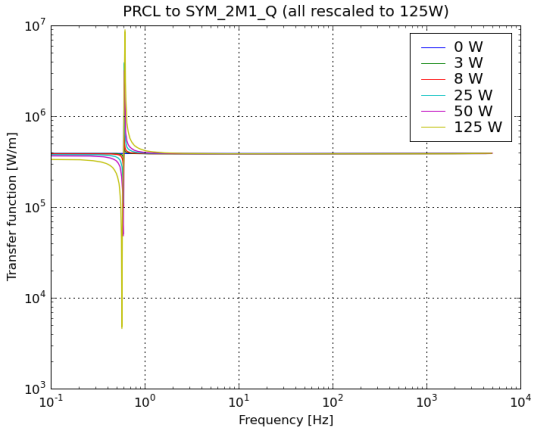
PRCL to SYM_2M1_Q (all rescaled to 125W)
Transfer function [W/m]
Frequency [Hz]
0 W
3 W
8 W
25 W
50 W
125 W

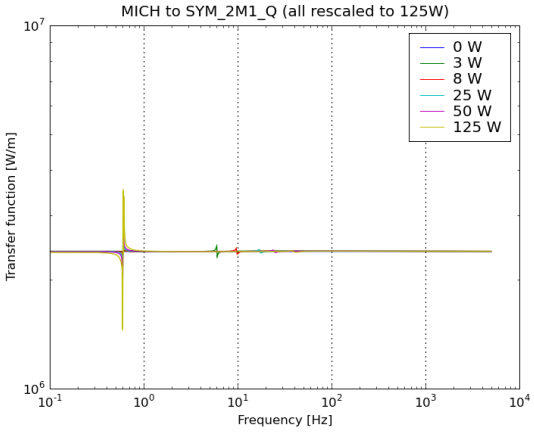
MICH to SYM_2M1_Q (all rescaled to 125W)
Transfer function [W/m]
Frequency [Hz]
0 W
3 W
8 W
25 W
50 W
125 W

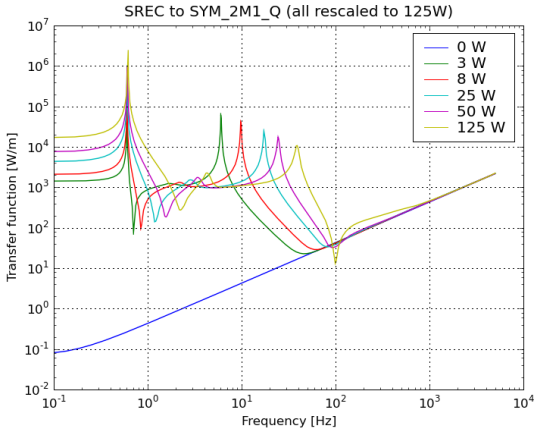
SREC to SYM_2M1_Q (all rescaled to 125W)
Transfer function [W/m]
Frequency [Hz]
0 W
3 W
8 W
25 W
50 W
125 W

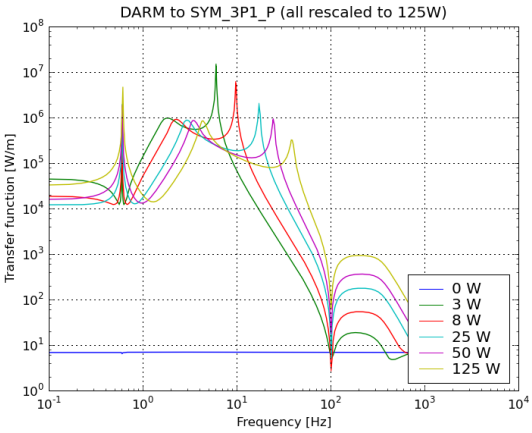
DARM to SYM_3P1_P (all rescaled to 125W)
Transfer function [W/m]
Frequency [Hz]
0 W
3 W
8 W
25 W
50 W
125 W

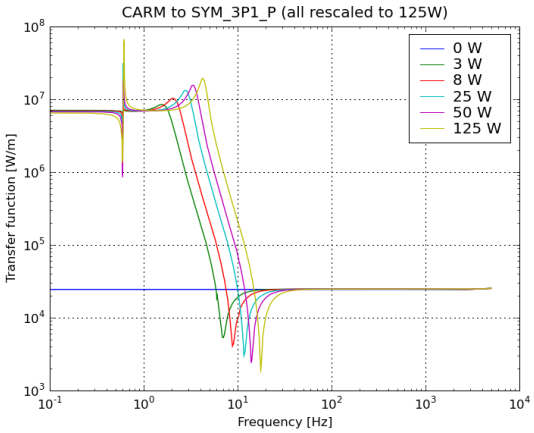
CARM to SYM_3P1_P (all rescaled to 125W)
Transfer function [W/m]
Frequency [Hz]
0 W
3 W
8 W
25 W
50 W
125 W

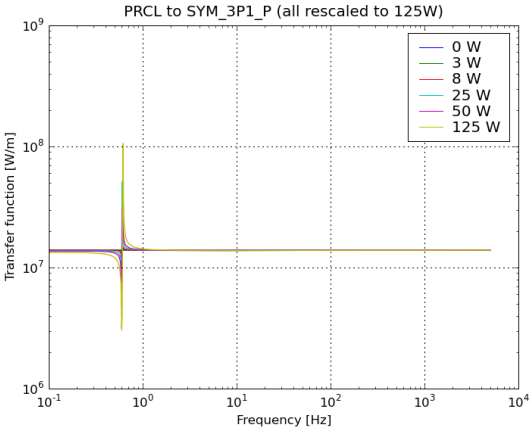
PRCL to SYM_3P1_P (all rescaled to 125W)
Transfer function [W/m]
Frequency [Hz]
0 W
3 W
8 W
25 W
50 W
125 W

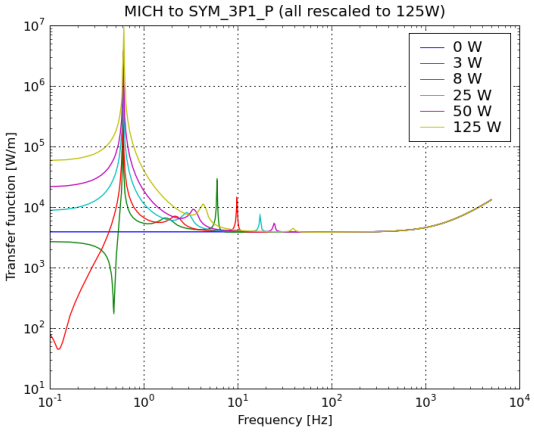
MICH to SYM_3P1_P (all rescaled to 125W)
Transfer function [W/m]
Frequency [Hz]
0 W
3 W
8 W
25 W
50 W
125 W

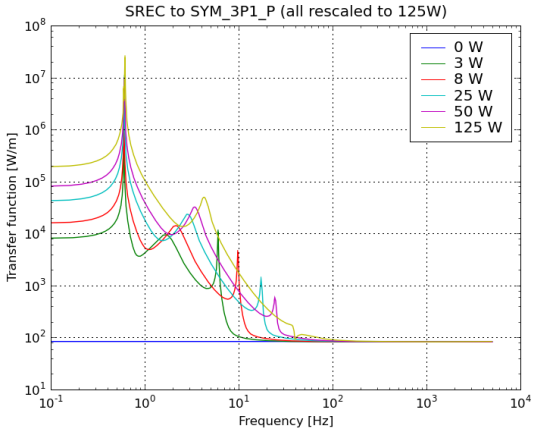
SREC to SYM_3P1_P (all rescaled to 125W)
Transfer function [W/m]
Frequency [Hz]
0 W
3 W
8 W
25 W
50 W
125 W

References

[1] G. Vajente, *"Note on Signal Recycling I: Field equations"*, VIR-030B-08 (2008) 2

[2] G. Vajente, *"Note on Signal Recycling II: Lengths and modulations"*, VIR-032A-08 (2008) 2

[3] G. Vajente, *"Simulation of Advanced Virgo Length Sensing and Control system"*, VIR-068A-08 (2008) 1, 2